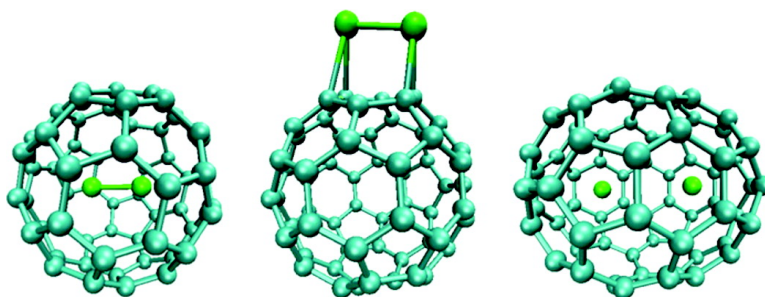Article

Is Fullerene C Large Enough to Host a Multiply Bonded Dimetal?

Ivan Infante, Laura Gagliardi, and Gustavo E. Scuseria

More About This Article

Additional resources and features associated with this article are available within the HTML version:

- Supporting Information
- Links to the 1 articles that cite this article, as of the time of this article download
- Access to high resolution figures
- Links to articles and content related to this article
- Copyright permission to reproduce figures and/or text from this article

View the Full Text HTML

Is Fullerene C_{60} Large Enough to Host a Multiply Bonded Dimetal?

Ivan Infante,[†] Laura Gagliardi,*,[†] and Gustavo E. Scuseria[‡]

Department of Physical Chemistry, University of Geneva, 30 Quai Ernest Ansermet, CH-1211 Geneva, Switzerland and Department of Chemistry, Rice University, Houston, Texas

Received February 2, 2008; E-mail: laura.gagliardi@chiphy.unige.ch

Abstract: Some dimetal fullerenes $M_2@C_{60}$ (M = Cr, Mo, W) have been studied with computational quantum chemistry methods. The transition metal diatomic molecules Cr_2, Mo_2, W_2 form exohedral complexes with C_{60}, while U_2 forms a highly symmetric endohedral compound and it is placed in the center of the C_{60} cavity. This highly symmetric structure is an artifact due to the small size of the C_{60} cavity, which constrains U_2 at the center. If a larger cavity is used, like C_{70} or C_{84}, U_2 preferentially binds the internal walls of the cavity and the U−U bond no longer exists.

Introduction

Metal−metal multiple bonds have first attracted the attention of chemists in the 1960s, when Cotton introduced the notion of a quadruple bond between two Re atoms in the $Re_2Cl_8^{2-}$ anion.[1] Five bonds followed in 2005, when the synthesis[2] of a complex organometallic compound was interpreted in terms of a quintuple bond between two chromium atoms.[3] To find the molecules with the highest bond order, Roos et al. investigated the transition metal dimers of chromium, molybdenum, and tungsten, respectively, Cr_2, Mo_2, and W_2, and suggested the presence of a hexuple bond in W_2.[4] Similar work has also been performed in the early diactinide series,[5–8] indicating that a well-developed quintuple bond occurs in Pa_2 and a strong quadruple bond occurs in U_2.

Endohedral metallofullerenes have been extensively studied since the discovery of fullerenes.[9,10] These systems present distinctive characteristics because the charge transfer induced by the metal with the cage can change the reactivity and properties of the fullerene itself. This aspect is particularly attractive for the potential new applications in both chemistry and medicine. Wilson et al.[11] have proposed a possible biomedical application of holmium fullerenes as a tracer in diagnostic radiology. One advantage of using fullerene cages, among many others, is the possibility to isolate completely the metal from the surrounding giving a very low toxicity. Unstable fullerene cages can be synthesized with a properly trapped metal also when the isolated-pentagon rule (IPR) is violated.[12–15] New electrochemical properties and reactivity can be detected. Recently, it has been shown experimentally how organic functional groups can react with a endohedral metallofullerene.[16,17] Even more interesting is the possibility to prepare new electronic devices, for which the electron transfer between the metal and the fullerene can be used to build special types of single-wall nanotubes.[18]

From a theoretical standpoint, it is interesting to understand how the metal binds to the fullerene. Some questions that one would like to address are as follows: does the metal energetically prefer to bind the cage from the outside or inside? How many metal atoms can be encapsulated, and how do they interact among themselves? Experimentalists have pushed the number of metal atoms that can reside inside a fullerene to three in the $M_3N@C_{80}$ (M = Sc, Y) species.[19] In this system the metal atoms are bonded to the nitrogen atom. Two metal atoms with no other interfering elements have been isolated inside a fullerene cage only recently. Examples like $Sc_2@C_{66}$, $La_2@C_{72}$, and $La_2@C_{78}$

† University of Geneva.
‡ Rice University.
(1) Cotton, F. A.; Harris, C. B. *Inorg. Chem.* **1965**, *4*, 330.
(2) Nguyen, T.; Sutton, A. D.; Brynda, S.; Fettinger, J. C.; Long, G. J.; Power, P. P. *Science* **2005**, *310*, 844.
(3) Brynda, M.; Gagliardi, L.; Widmark, P. O.; Power, P. P.; Roos, B. O. *Angew. Chem., Int. Ed.* **2006**, *45*, 3804.
(4) Roos, B. O.; Borin, A. C.; Gagliardi, L. *Angew. Chem., Int. Ed.* **2007**, *46*, 1469.
(5) Roos, B. O.; Gagliardi, L. *Inorg. Chem.* **2006**, *45*, 803.
(6) La Macchia, G.; Brynda, M.; Gagliardi, L. *Angew. Chem., Int. Ed.* **2006**, *45*, 6210.
(7) Gagliardi, L.; Roos, B. O. *Nature* **2005**, *433*, 848.
(8) Gagliardi, L.; Pyykko, P.; Roos, B. O. *Phys. Chem. Chem. Phys.* **2005**, *7*, 2415.
(9) Heath, J. R.; Obrien, S. C.; Zhang, Q.; Liu, Y.; Curl, R. F.; Kroto, H. W.; Tittel, F. K.; Smalley, R. E. *J. Am. Chem. Soc.* **1985**, *107*, 7779.
(10) Kroto, H. W.; Heath, J. R.; Obrien, S. C.; Curl, R. F.; Smalley, R. E. *Nature* **1985**, *318*, 162.

(11) Wilson, L. J.; Cagle, D. W.; Thrash, T. P.; Kennel, S. J.; Mirzadeh, S.; Alford, J. M.; Ehrhardt, G. J. *Coord. Chem. Rev.* **1999**, *199*, 190.
(12) Wang, C.; Kai, T.; Tomiyama, T.; Yoshida, T.; Kobayashi, T.; N. E.; Takata, M.; Sakata, M.; Shinohara, H. *Nature* **2000**, *408*, 426.
(13) Stevenson, S.; Fowler, P. W.; Heine, T.; Duchamp, J.; Rice, G.; Glass, T.; Harich, K.; Hadju, E.; Bible, R.; Dorn, H. C. *Nature* **2000**, *408*, 427.
(14) Shi, Z.; Wu, X.; Wang, C.; Lu, X.; Shinohara, H. *Angew. Chem., Int. Ed.* **2006**, *45*, 2107.
(15) Kato, H.; Taninaka, A.; Sugai, T.; Shinohara, H. *J. Am. Chem. Soc.* **2003**, *125*, 7782.
(16) Yamada, M.; Wakahara, Y.; Lian, Y.; Tsuchiya, T.; Waelchli, M.; Mizorogi, N.; Nagase, S.; Kadish, K. M. *J. Am. Chem. Soc.* **2006**, *128*, 1400.
(17) Yamada, M.; Wakahara, Y.; Nakahodo, T.; Tsuchiya, T.; Maeda, Y.; Akasaka, T.; Yoza, T.; Horn, E.; Mizorogi, N.; Nagase, S. *J. Am. Chem. Soc.* **2006**, 128.
(18) Di Ventra, M.; Evoy, S.; Heflin, J. R. *Introduction to Nanoscale Science and Technology*; Springer: 2004.

can now be found in the literature.[20–22] Up to now, however, the idea that a real metal−metal bond could form inside a fullerene remains fascinating and not demonstrated yet.

Wu and Lu[23] have recently shown that by means of all-electron relativistic density functional calculations $U_2@C_{60}$ has an unprecedented U−U multiple bond consisting solely of sixfold ferromagnetically coupled one-electron-two-center bonds. The electronic configuration is $(5f\pi_u)^2(5f\sigma_g)^1(5f\delta_g)^2(5f\varphi_u)^1$, and the bonds are dominated by the uranium 5f atomic orbitals. The authors described this work as the first connection between metal−metal multiple bonding chemistry and fullerene chemistry.

We present here the results of a computational study of several species with the general formula $M_2@C_{60}$, where the dimetal $M_2 = Cr_2$, Mo_2, W_2, and U_2 resides inside and outside the fullerene cage. We decided to choose these elements because they all present the same number of valence electrons and, in principle, they could reach maximum bond multiplicity. Moreover, the uranium atom has the 5f shell that actively participates in the formation of the dimetal bond and can give origin to a new type of chemical interaction with the cage.

Local minima were characterized by vibrational frequency analysis. The relative stabilities of the different species were compared, and the nature of the metal−metal multiple bond and its interaction with the cage was analyzed. For the U_2 dimer, we also explored the possibility of forming endohedral complexes with the C_{70} and C_{84} cages.

Theoretical Methods

Quantum chemical calculations were performed using density functional theory (DFT). The TURBOMOLE package[24] was employed. Scalar relativistic effects were incorporated by employing on the uranium atom the (14s13p10d8f3g)/[10s9p5d4f3g] ECP basis set with 60 core−electrons.[25] A valence double-ζ split valence basis set, SVP,[26] was used on the carbon atoms. The gradient-corrected BP86[27] exchange correlation (xc) functional was employed. Some of the calculations were also repeated using the PBE[28] and PBE0[29,30] xc-functionals. The choice of the functionals was based on previous work,[31–33] which showed that pure DFT methods perform better than hybrid DFT or many-body perturbation methods in describing metal diatomics.

Full geometry optimization and frequency calculations were performed for all the C_{60} species. The threshold for the energy gradient has been chosen as 10^{-4}. Basis set superposition error

(BSSE) corrections were included using the counterpoise method. Zero-point energy corrections (ZPE) were also computed. For the most stable C_{70} and C_{84} structures, we followed a "steepest descent" procedure to ensure that we were in a minimum region. A full frequency calculation was not performed for the larger clusters; hence ZPE energy corrections were not computed for these systems. The method has proven to be successful for similar compounds.[34–36]

We have studied the interaction between the fullerene and the dimetal by classifying the energy of the $M_2@C_n$ systems in a series of contributions. The bonding energy, ΔE_{bond}, between two fragments is expressed as the sum of two terms, one destabilizing term called strain energy or preparation energy, ΔE_{strain} (the two expressions will be used as synonyms in the following), and one stabilizing term called interaction energy, ΔE_{int}: $\Delta E_{bond} = \Delta E_{strain} + \Delta E_{int}$. ΔE_{strain} is associated with the deformation of the individual fragments when they form the supersystem. This contribution is always positive, and its magnitude depends on the rigidity and reorganization of each fragment. ΔE_{int} is the effective interaction between the deformed fragments. The terms that appear in the total binding energy expression are evaluated in the following way:

$$\Delta E_{int}(M_2@C_n) = E(M_2@C_n) - E(M_2)[\text{in } M_2@C_n] -$$
$$E(C_n)[\text{in } M_2@C_n]$$

$$\Delta E_{strain} = E(M_2)[\text{in } M_2@C_n] - E(M_2) + E(C_n)[\text{in } M_2@C_n] - E(C_n)$$

In the following we will refer to the first term as encapsulation energy, when the dimetal is inside the cage, or complexation energy, when the dimetal is attached from the outside.

To analyze the charge transfer between the metal atoms and the fullerene fragments we used natural population charges[37] as implemented in TURBOMOLE.

Results and Discussion

Structure. The metal−metal bond distances in the metal diatoms M_2 (M = Cr, Mo, W, U) are reported in Table 1, together with the relative stability of the lowest electronic states. For each dimetal, several $M_2@C_{60}$ structures were considered, namely M_2 inside C_{60} (Structure **1a** and **1b**), M_2 outside C_{60} (Structure **2**), and the two metal atoms separated and attached at opposite sides of the cage (Structure **3**). All possible structures are depicted in Figures 1–3. The results on the $M_2@C_{60}$ systems are summarized in Table 2. The most significant bond distances for each structure are reported, together with the relative stability of the structures.

The most stable structure for $Cr_2@C_{60}$ is the exohedral one, in which Cr_2 lies on one side of C_{60} (Structure **2**) and the Cr−Cr bond distance is considerably elongated with respect to the isolated Cr_2 molecule. The singlet and triplet lowest states are close in energy. With the inclusion of the zero-point energy (ZPE) and BSSE corrections, BP86 predicts the singlet ^1A state to lie ∼4 kcal/mol lower in energy than the triplet ^3A state. PBE without ZPE and BSSE corrections gives the same results as BP86 without ZPE and BSSE. If one thus corrects the PBE results using the BP86 ZPE and BSSE corrections, one can conclude that the two functionals give very similar results. The Cr−Cr bond distance in the ^1A state is 2.62 and 2.42 Å in the ^1A and ^3A states, respectively, at both levels of theory. The structure with two Cr atoms lying outside C_{60} (Structure **3**), but on opposite sides of the C_{60} wall, is higher in energy than

(19) Stevenson, S.; Rice, G.; Glass, T.; Harich, K.; Cromer, F.; Jordan, M. R.; Craft, J.; Hadju, E.; Bible, R.; Olmstead, M. M.; Maltra, K.; Fisher, A. L.; Balch, A. L.; Dorn, H. C. *Nature* **1999**, *401*, 55.

(20) Kato, H.; Taninaka, A.; Sugai, T.; Shinohara, H. *J. Am. Chem. Soc.* **2003**, *125*, 7782.

(21) Cao, B.; Nikawa, H.; Nakahodo, T.; Tsuchiya, T.; Maeda, Y.; Akasaka, T.; Sawa, H.; Slanina, Z.; Mizorogi, N.; Nagase, S. *J. Am. Chem. Soc.* **2008**, *130*, 983.

(22) Shi, Z.-Q.; Wu, X.; Wang, C.-R.; Lu, X.; Shinohara, H. *Angew. Chem., Int. Ed.* **2006**, *45*, 2107.

(23) Wu, X.; Lu, X. *J. Am. Chem. Soc.* **2007**, *129*, 2171.

(24) Ahlrichs, R.; Bar, M.; Haser, M.; Horn, H.; Kolmel, C. *Chem. Phys. Lett.* **1989**, *162*, 165.

(25) Cao, X. Y.; Dolg, M. *THEOCHEM* **2004**, *673*, 203.

(26) Schafer, A.; Horn, H.; Ahlrichs, R. *J. Chem. Phys.* **1992**, 97.

(27) Perdew, J. P. *Phys. Rev. B* **1986**, *33*, 8822.

(28) Perdew, J. P.; Burke, K.; Ernzerhof, M. *Phys. Rev. Lett.* **1996**, *77*, 3865.

(29) Ernzerhof, M.; Scuseria, G. E. *J. Chem. Phys.* **1999**, *110*, 5029.

(30) Adamo, C.; Barone, V. *J. Chem. Phys.* **1999**, *110*, 6158.

(31) Yanasigava, S.; Tsuneda, T.; Hirao, K. *J. Chem. Phys.* **2000**, *112*, 545.

(32) Barden, C. J.; Rienstra-Kiracofe, J. C.; Schaefer, H. F. *J. Chem. Phys.* **2000**, *113*, 690.

(33) Gutsev, G. L.; Charles, W.; Bauschlicher, J. *J. Phys. Chem. A* **2003**, *107*, 4755.

(34) Gagliardi, L.; Heaven, M. C.; Krogh, J. W.; Roos, B. O. *J. Am. Chem. Soc.* **2005**, *127*, 86.

(35) Hagberg, D.; Karlstrom, G.; Roos, B. O.; Gagliardi, L. *J. Am. Chem. Soc.* **2005**, *127*, 14250.

(36) Gagliardi, L.; Willetts, A.; Skylaris, C. K.; Handy, N. C.; Spencer, S.; Ioannou, A. G.; Simper, A. M. *J. Am. Chem. Soc.* **1998**, *120*, 11727.

(37) Reed, A. E.; Curtiss, L. A.; Weinhold, F. *Chem. Rev.* **1988**, *88*, 899.

Table 1. Dissociation Energy ($D_e = E(M_2) - 2E(M)$) for the Cr_2, Mo_2, W_2, and U_2 Systems in Various Electronc States[a]

system	el. state	method	R_{eq}	D_e (kcal/mol)	ΔE (kcal/mol)
Cr_2	^1A	BP86	1.62	−23.4	0.0
		PBE	1.62	−24.3	0.0
		CASPT2	1.66	−38.1	--
	^3A	BP86	1.76	−8.2	15.2
		PBE	1.76	−7.9	16.4
Mo_2	^1A	BP86	1.98	−75.0	0.0
		PBE	1.98	−76.7	0.0
		CASPT2		−119.7	
	^3A	BP86	2.09	−54.5	21.6
		PBE	2.08	−55.1	20.6
W_2	^1A	BP86	2.07	−117.5	0.0
		PBE	2.07	−123.0	0.0
		CASPT2		−146.9	
	^3A	BP86	2.14	−111.2	6.2
		PBE	2.14	−115.6	7.4
U_2	^5A	BP86	2.30	−70.1	0.3
		PBE	2.29	−75.8	0.0
	^7A	BP86	2.36	−70.1	0.3
		PBE	2.36	−75.2	0.6
		CASPT2		−32.6	
	^9A	BP86	2.43	−70.4	0.0
		PBE	2.43	−74.8	0.9

[a] Energy difference (ΔE) between different electronic states. The DFT results are from the present study. The CASPT2 results are from ref 4.

structure **2**. In the endohedral arrangement, the Cr−Cr bond is significantly longer than that in an isolated Cr_2 molecule (1.62 Å). The two Cr atoms can assume two different positions depending on the spin multiplicity of the complex. For the singlet state the Cr atoms are not in the center of the cage but rather attached to the internal wall of C_{60} (Structure **1a**), while in the triplet state the metal atoms are more centered in the cage (Structure **1b**). The same pattern is found for Mo and W.

In the $Mo_2@C_{60}$ case, the exohedral structure (Structure **2**) is also the most stable one, and it corresponds to a triplet ground state. The Mo−Mo bond distance is 2.16 Å. The ground state of isolated Mo_2 is a singlet state with a Mo−Mo bond distance of 1.98 Å, while the triplet Mo_2 state has a Mo−Mo bond distance of 2.14 Å. $W_2@C_{60}$ also prefers the exohedral arrangement (**2**). The lowest singlet and triplet are very close in energy. The W−W bond distance is 2.27 Å for both states, while in isolated W_2 it is 2.07 and 2.14 Å for the singlet and triplet, respectively.

Inspection of Table 2 shows that the situation is significantly different in the $U_2@C_{60}$ case. As already pointed out by Wu and Lu, the most favorite structure is the endohedral one (Structure **1**). U_2 lies at the center of the cage, the system is highly symmetric, and the U−U bond distance is 2.73 Å. This value is significantly longer than that in isolated U_2 (2.3−2.4 Å, according to various levels of theory), but one can still consider the U_2 as a unit. Moreover, according to all DFT levels of theory, endohedral $U_2@C_{60}$ is very stable with respect to separated U_2 and C_{60}. Wu and Lu[23] attributed this stability to a favorable interaction between the 5f orbitals of U and the C_{60} orbitals. Earlier theoretical/experimental studies[38,39] had indicated very strong binding between U and small fullerene cages

(38) Guo, T.; Diener, M. D.; Chai, Y.; Alford, M. J.; Haufler, R. E.; McClure, S. M.; Ohno, T.; Weaver, J. H.; Scuseria, G. E.; Smalley, R. E. *Science* **1992**, *257*, 1661.
(39) T. Guo, R. E.; Smalley, T; Scuseria, G. E. *J. Am. Chem. Soc.* **1993**, *99*, 352.

as opposed to charge transfer.[40] Our previous studies on metal diatomics[4] indicated that there are some differences between transition metal diatomics (for example Cr_2, Mo_2, and W_2) and actinide diatomics, but these difference do not seem to justify why U_2 would prefer the symmetrical endohedral conformation, while all the transition metal diatomics have a clear preference for either the exohedral structure or an endohedral structure in which the M_2 fragment is considerably elongated with respect to the isolated molecule and attached to the C_{60} wall. In order to understand this difference, we have performed a bond analysis.

Bond Analysis. The stability of the endohedral and exohedral structures can be expressed as the difference between the total energy of the complexes and the energy of their components, namely M_2 and C_{60} (or C_{72} or C_{84}). Encapsulation and complexation energy terms can be decomposed in several contributions as shown in Table 3.

When forming the $M_2@C_{60}$ supercomplex, a considerable charge transfer between M_2 and C_{60} occurs. However, for simplicity in our model, we assume that the strain energy term includes only the effect of the geometrical distortion. In other words, we assume that M_2 and C_{60} have the same electronic configuration in the supercomplex as when they are isolated species. In such a way, all the electronic effects are included in the interaction energy term. This analysis was performed only on the closed-shell electronic states. The reason was that the metal/fullerene coordination does not depend on the spin multiplicity, because the energy difference between singlet and triplet for a given supercomplex is significantly smaller than the energy difference between the endohedral and exohedral structures.

The Cr_2 endohedral complex presents an encapsulation energy of −2.7 kcal/mol. This small value is a consequence of the small interaction energy between the two fragments, −9.2 kcal/mol. Neither the metal−metal bond nor the fullerene cage undergoes any major deformation in the supercomplex. The fullerene cage is destabilized by ∼6 kcal/mol. In the exohedral structure, the preparation energy of Cr_2 is very large, namely 154 kcal/mol, which is reflected in the strong elongation of the Cr−Cr distance. In the exohedral complex, the Cr atoms strongly interact with the fullerene cage, which is more deformed than in the endohedral case. The encapsulation energy is −36 kcal/mol, but the effective interaction energy between the incarcerated dimetal and the cage is ∼200 kcal/mol. This large number also includes the strong electronic rearrangement (polarization) within the dimetal fragment as a consequence of the effective rupture of the Cr−Cr bond. To make more evident this aspect, in Table 4 we added the natural electronic configurations of the Cr atom in the endohedral and exohedral structures as compared to the case of the isolated Cr_2 molecule. In Cr_2, Cr assumes the $4s^13d^5$ electronic configuration, while in the endohedral system each Cr atom is depleted of ∼0.50−0.55 electrons, which corresponds to the total amount of charge that is transferred to the fullerene cage, 1.1 electrons, as shown in Table 5. For the more stable exohedral complex, the total electron charge transfer from the dimetal to the cage is of about 1.3 electrons. This value, slightly larger than that in the endohedral case, does not explain the electronic configuration of the Cr atoms, $4s^{0.09}3d^{5.23}$, which seems more related to a large polarization effect from the 4s to the 3d orbitals.

(40) Wang, L. S.; Alford, J. M.; Chai, Y; Diener, M.; Zhang, J.; McClure, S. M.; Guo, T.; Smalley, R.; E.Scuseria, G. E. *Chem. Phys. Lett.* **1993**, *207*, 354.
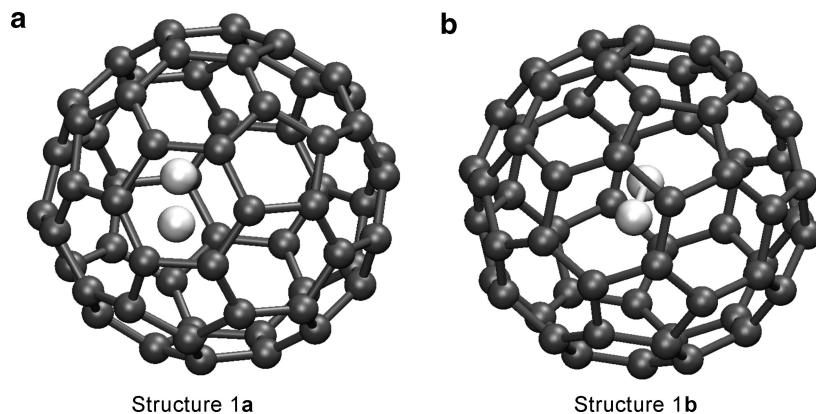
a

Structure 1**a**

b

Structure 1**b**

Figure 1. Two possible endohedral arrangements of $M_2@C_{60}$.

Structure **2**

Figure 2. Exohedral arrangement of $M_2@C_{60}$.
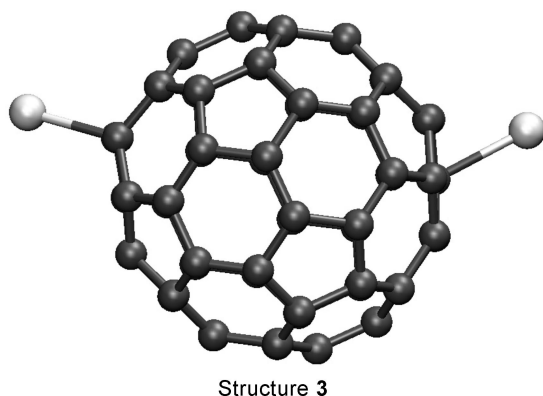

Structure **3**

Figure 3. Structure of two metal atoms attached to the external walls of C_{60}.

The Mo_2 complexes show an encapsulation energy that resembles the Cr_2 ones, and the exohedral structure is more stable than the endohedral structure. Their energy decomposition however is different compared to the Cr_2 cases. The preparation energy of Mo_2 for the endohedral complex, 83.8 kcal/mol, is larger than in the Cr_2 case, indicating that the Mo–Mo bond distance is more elongated than when the Mo atoms are outside the cage. In this latter case the deformation energy is only 14.0 kcal/mol. Such an effect determines also a large deformation (preparation) of the fullerene for the endohedral complex, of about 37.5 kcal/mol with respect to the isolated icosahedral C_{60}. In the exohedral complex the fullerene deformation is only 10.2

kcal/mol. The position of the Mo atoms allows a large interaction in the endohedral complex, which is also reflected by a large charge transfer "guest-to-host", of ∼1.3 electron, compared to 0.8 electron, in the exohedral complex. To summarize, while the interaction energy is more favorable for the endohedral complex (with respect to the exohedral), the strain energy, to bring the fragments in the geometry they assume in the supersystem, quenches completely this effect by making the complex unstable and unlikely to form. On the other hand, the exohedral complex, despite a smaller charge rearrangement, is stable.

The W_2 systems show similar features to the Mo_2 systems. A charge transfer from W_2 to the cage of ∼1.3 electrons and 0.9 electron, respectively, occurs in the endohedral and exohedral systems, respectively. As for Cr_2, also for W_2, the exohedral molecule has an overall larger stabilization energy.

When U_2 is used as a guest, the interaction pattern changes dramatically. The endohedral complex is the most stable structure with an encapsulation energy of ∼ −207 kcal/mol. The exohedral structure, with a complexation energy of only −73 kcal/mol, is still more stable than in the Cr, Mo and W case. To understand the origin of such a different behavior, we have analyzed the bonding decomposition of the endohedral and exohedral complexes. The preparation energy of U_2 is rather small for both structures, but it presents a larger deformation in the endohedral complex. The elongation of the U–U bond distance is larger inside the cage than outside, indicating that the uranium atoms tend to stay bound to each other when they are not encapsulated. Looking at the amount of charge transfer between U_2 and the cage, the endohedral system shows a flow of ∼4.4 electron, which is almost double with respect to the exohedral complex, 2.5 electrons. Compared to the other systems the charge transfer is ∼4 times larger The natural population charge, performed on the isolated U_2 molecule, gives the following electronic distribution on each uranium atom: $7s^{1.15}6d^{1.65}5f^{3.13}7p^{0.07}$. On the other hand, in $U_2@C_{60}$, each U atom has the following electronic distribution: $7s^{0.01}6d^{0.59}5f^{3.11}7p^{0.04}$. In going from isolated U_2 to $U_2@C_{60}$ the 7s orbital is totally emptied, and also the occupation of the 6d orbital is strongly reduced. The 5f orbital seems not to participate in the bond. This result is in agreement with the suggestion of Wu and Lu[23] that, inside the fullerene, the U_2 electron transfer involves the 7s and 6d orbitals. When U_2 is outside the cage, the charge transfer is not as dramatic. The 7s and 6d U orbitals are responsible for the interaction with a transfer of ∼1.1 electrons per uranium atom, but this time also the 5f orbitals participate actively with 0.13 electron. The U_2

Table 2. $M_2@C_{60}$: Typical Bond Distances (Å) and Encapsulation/Complexation Energies (kcal/mol) for Various Electronic States

system	el. state	structure	method	main bond distances (Å) M—M	M—C	De (kcal/mol)
$Cr_2@C_{60}$	^1A	**1a**	BP86	1.61	2.37	−2.7
			+ZPE			−4.8
			PBE	2.74	2.48	−9.8
	^3A	**1b**	BP86	2.44	2.23	−10.9
			+ZPE			−14.9
			PBE	2.54	2.20	−17.1
	^1A	**2**	BP86	2.61	2.10	−36.2
			+ZPE			−38.0
			+BSSE			−34.4
			PBE	2.62	2.09	−38.2
			PBE0	2.86	2.18	−19.3
	^3A	**2**	BP86	2.42	2.45	−37.1
			+ZPE			−38.4
			+BSSE			−29.6
			PBE	2.42	2.41	−38.8
			PBE0	2.70	2.12	−20.6
	^1A	**3**	BP86	10.75	2.25	−18.8
			+ZPE			−21.3
			PBE	10.72	2.23	−19.7
	^3A	**3**	BP86	10.74	2.23	−11.8
			+ZPE			−14.8
			PBE	10.71	2.22	−12.9
$Mo_2@C_{60}$	^1A	**1a**	BP86	2.56	2.10	23.3
			+ ZPE			20.4
			PBE	2.67	2.07	8.7
			PBE0	2.67	2.07	−5.7
	^3A	**1b**	BP86	1.95	2.62	24.8
			+ZPE			21.6
			PBE	1.94	2.64	16.9
			PBE0	2.01	2.62	−8.8
	^1A	**2**	BP86	2.16	2.36	−28.1
			+ZPE			−29.5
			+BSSE			−24.9
			PBE	2.16	2.34	−31.5
			PBE0	2.24	2.37	−49.3
	^3A	**2**	BP86	2.16	2.43	−32.8
			+ZPE			−33.2
			+BSSE			−29.7
			PBE	2.16	2.40	−36.1
			PBE0	2.25	2.56	−56.5
	^1A	**3**	BP86	10.81	2.18	37.3
			+ZPE			34.6
			PBE	10.79	2.17	36.2
	^3A	**3**	BP86	10.92	2.30	41.4
			+ZPE			39.0
			PBE	10.89	2.29	40.7
$W_2@C_{60}$	^1A	**1a**	BP86	2.54	2.26	27.7
			+ZPE			23.9
			PBE	2.68	2.15	10.9
	^3A	**1b**	BP86	2.34	2.25	30.3
			+ZPE			26.4
			PBE	2.36	2.25	19.3
	^1A	**2**	BP86	2.27	2.28	−40.3
			+ZPE			−41.2
			+BSSE			−37.6
			PBE	2.26	2.27	−44.2
			PBE0	2.39	2.12	−67.1
	^3A	**2**	BP86	2.27	2.38	−43.6
			+ZPE			−44.3
			+BSSE			−36.1
			PBE	2.26	2.35	−47.3
			PBE0	2.30	2.50	−63.4
	^1A	**3**	BP86	10.68	2.09	123.3
			+ZPE			120.0
			PBE	10.67	2.09	120.4
	^3A	**3**	BP86	10.77	2.12	75.9
			+ZPE			
			PBE	10.76	2.12	74.5
$U_2@C_{60}$	^5A	**1b**	BP86	2.55	2.52	−200.9
			PBE	2.56	2.50	−221.3
	^7A	**1b**	BP86	2.73	2.48	−207.4

Table 2. Continued

system	el. state	structure	method	main bond distances (Å) M–M	M–C	De (kcal/mol)
			ZPE			−212.1
			BSSE			−201.3
			PBE			−228.0
			PBE0	2.67	2.49	−198.7
	^9A	**1b**	BP86	2.70	2.46	−195.1
			PBE	2.72	2.49	−213.6
	^5A	**2**	BP86	2.32	2.49	−72.1
			PBE	2.32	2.37	−83.0
	^7A	**2**	BP86	2.41	2.46	−73.3
			PBE	2.40	2.44	−78.8
	^9A	**2**	BP86	2.58	2.36	−74.7
			PBE	2.57	2.35	−79.5

Table 3. Bonding Decomposition Scheme (kcal/mol) for the $M_2@C_n$ [M = Cr, Mo, W, U; n = 60, 70, 84] Molecules at the BP86/SV(P) Level of Theory

	Cr		Mo		W		$U(C_{60})$		$U(C_{70})$		$U(C_{84})$	
	in	out	in	out	in	out	in	out	in	out	in	out
prep M_2	0.1	154.0	83.8	14.0	64.6	16.9	15.3	27.8	85.2	8.5	81.2	1.3
prep C_{60}	6.4	10.2	37.5	10.2	35.2	14.2	20.7	9.0	24.7	9.2	15.8	19.0
interaction M_2–C_{60}	−9.2	−200.5	−98.1	−52.4	−72.2	−71.4	−243.3	−110.1	−308.2	−100.6	−257.8	−94.4
binding energy	−2.7	−36.2	23.2	−28.1	27.7	−40.3	−207.4	−73.3	−198.3	−82.9	−160.8	−74.0

Table 4. Natural Population Charges and Natural Electronic Conurations Computed at the DFT/BP86/SV(P) Level of Theory for the Metal Atoms in Different Molecular Fragments[a]

molecular system	Cr	Mo	W	U
M	$4s^1 3d^5$	$5s^1 4d^5$	$6s^2 5d^4$	$7s^2 6d^{1} 5f3$
M_2	$4s^1 3d^5$	$5s^1 4d^5$	$6s^1 5d^5$	$7s^{1.15} 6d^{1.65} 5f^{3.13} 7p^{0.07}$
$M_2@C_{60}$ (endohedral)	$4s^{0.59} 3d^{4.87}$	$5s^{0.13} 4d^{5.17}$	$6s^{0.65} 5d^{4.58}$	$7s^{0.01} 6d^{0.59} 5f^{3.11} 7p^{0.04}$
$M_2@C_{60}$ (exohedral)	$4s^{0.09} 3d^{5.23}$	$5s^{0.61} 4d^{4.98}$	$6s^{0.88} 5d^{4.68}$	$7s^{0.43} 6d^{1.31} 5f^{2.98} 7p^{0.06}$
$M_2@C_{70}$ (endohedral)	--	--	--	$7s^{0.15} 6d^{0.39} 5f^{2.90} 7p^{0.15}$
$M_2@C_{70}$ (exohedral)	--	--	--	$7s^{0.41} 6d^{1.01} 5f^{3.12} 7p^{0.05}$
$M_2@C_{84}$ (endohedral)	--	--	--	$7s^{0.23} 6d^{0.375} 5f^{3.00} 7p^{0.19}$
$M_2@C_{84}$ (exohedral)	--	--	--	$7s^{0.46} 6d^{1.21} 5f^{3.04} 7p^{0.05}$

[a] Only the major contributions are shown in the table. In M_2C_n [M = Cr, Mo, W, U; n = 60, 70, 84] with M_2 inside or outside the cage, the electronic configuration for a given metal is averaged over both the metal atoms.

Table 5. Total Amount of Charge Transferred from the Metal Atoms to the Fullerene Cage in the Endohedral and Exohedral M_2C_n [M = Cr, Mo, W, U; n = 60, 70, 84] Computed with a Natural Population Analysis at the DFT/BP86/SVP Level of Theory

	Cr	Mo	W	U
$M_2@C_{60}$ (endohedral)	1.09	1.26	1.32	4.43
$M_2@C_{60}$ (exohedral)	1.29	0.84	0.91	2.47
$M_2@C_{70}$ (endohedral)	--	--	--	4.69
$M_2@C_{70}$ (exohedral)	--	--	--	2.83
$M_2@C_{84}$ (endohedral)	--	--	--	4.33
$M_2@C_{84}$ (exohedral)	--	--	--	2.54

Table 6. $U_2@C_n$ (n = 70, 84): $M_2@C_{60}$: Typical Bond Distances (Å) and Encapsulation/Complexation Energies (kcal/mol) for Various Electronic States Computed at the BP86/SVP Level of Theory

structure	el. state	structure	main bond distances (Å) M–M	M–C	D_e
$U_2@C_{70}$	^5A	endohedral	3.99	2.38	−194.6
	^7A	endohedral	3.92	2.40	−198.3
	^9A	endohedral	3.70	2.41	−179.6
	^5A	exohedral	2.60	2.50	−70.2
	^7A	exohedral	2.58	2.45	−77.6
	^9A	exohedral	2.58	2.48	−82.9
$U_2@C_{84}$	^7A	endohedral	4.07	2.44	−160.9
	^7A	exohedral	2.44	2.40	−74.0

and C_{60} energy levels in both the endohedral and exohedral fragments in the supercomplex are very similar; thus one can suggest that most of the charge transfer from the U_2 inside the cage occurs because of a more favorable overlap between the diffuse 7s and 6d orbitals with the carbon orbitals. This overlap is so large that it compensates for the electrostatic repulsion of the two uranium atoms, with a charge of +2.2 each. Outside the cage this repulsion is quenched by the lower charge transfer; thus the two atoms, in a +1 formal charge, can actually bind to each other. From this analysis, it is evident that the formation of the U–U bond inside the C_{60} is an artifact due to the constraining size of the cage, rather than an actual bond.

To verify this latter point, we decided to perform benchmark calculations on U_2 in larger cages, namely C_{70} and C_{84}. The results are summarized in Table 6.

The ground state of $U_2@C_{70}$ is the ^7A heptet state. The endohedral structure is still energetically more favorable than the exohedral structures. However, U_2 does not lie at the center of the cage, the U–U bond distance is considerably longer, 3.91 Å, and the U–C distance is 2.40 Å. In C_{84} we explored the heptet state only, since from the analysis reported above it is evident that the spin multiplicity has a negligible contribution

in determining the stabilization of the endohedral structure with respect to the exohedral structure. In this case U_2 is even less constrained and the U−U distance is 4.07 Å. The energy analysis for the C_{70} and C_{84} systems gives similar results to those reported for the C_{60} cage, in terms of interaction energies and charge transfer.

Conclusions

We have presented the results of a DFT study on endohedral and exohedral $M_2@C_{60}$ systems, where M = Cr, Mo, W, U. In the endohedral $Cr_2@C_{60}$ only a small interaction occurs between Cr_2 and C_{60}, which do not undergo any major deformation. In the exohedral complex the Cr atoms interact more strongly with the fullerene cage, and an overall major deformation occurs. The exohedral complex is more stable than the endohedral complex.

Also in the Mo_2 and W_2 cases the exohedral structure is more stable than the endohedral structure. The U_2 case is different, in the sense that the endohedral complex is significantly more stable than the exohedral one and U_2 lies at the center of the cage. This result could lead to the wrong belief that a bond still occurs between the two U atoms. We have shown that this is an artifact due to the small size of the cage. In a larger cage such as, for example, C_{70} or C_{84}, the U−U distance becomes significantly longer, 3.9−4.0 Å, than that in the isolated U_2 molecule, 2.40 Å, and U_2 is not at the center of the cage any longer, but instead the two U atoms interact with the interior wall of the cage.

Supporting Information Available: Cartesian coordinates for all species and tables of calculated frequencies. This material is available free of charge via the Internet at http://pubs.acs.org.

JA800847J